Dicationic Diarylfurans as Anti-*Pneumocystis carinii* Agents

David W. Boykin,*,† Arvind Kumar,† Jaroslaw Spychala,† Min Zhou,† Richard J. Lombardy,† W. David Wilson,† Christine C. Dykstra,‡ Susan K. Jones,‡ James E. Hall,‡ Richard R. Tidwell,‡ Charles Laughton,§ Christine M. Nunn,§ and Stephan Neidle§

Department of Chemistry and Center for Biotechnology and Drug Design, Georgia State University, Atlanta, Georgia 30303, Department of Pathology, School of Medicine, The University of North Carolina at Chapel Hill, Chapel Hill, North Carolina 27599, and CRC Biomolecular Structure Unit, The Institute of Cancer Research, Sutton, Surrey SM2 5NG, U.K.

Received October 21, 1994®

Seven dicationic 2,5-diarylfurans have been synthesized, and their interactions with poly(dA-dT) and the duplex oligomer d(CGCCAATTCGCG)$_2$ were evaluated by T_m measurements. The inhibition of topoisomerase II isolated from *Giardia lamblia*, the inhibition of growth of *G. lamblia* in cell culture by these furans, and the effectiveness of these compounds against *Pneumocystis carinii* in the immunosuppressed rat model have been assessed. Strong binding affinities to poly(dA-dT) and to the oligomer were observed for the dicationic furans, and the interaction strength is directly correlated to the biological activity of the compounds. An X-ray structure for the complex of the dicationic amidine derivative, 2,5-bis(4-guanylphenyl)furan (**1**), with the oligomer demonstrates the snug fit of these compounds with the AATT minor-groove binding site and hydrogen bonds to AT base pairs at the floor of the minor groove. The stronger DNA binding molecules are the most effective inhibitors of topoisomerase II and *G. lamblia* in cell culture, and there is a correlation for both DNA interaction and topoisomerase II inhibition with the biological activity of these compounds against *G. lamblia*. Compound **1** is the most effective against *P. carinii*, it is more active and less toxic than pentamidine on intravenous administration and it is also effective by oral dosage. The results presented here suggest a model for the biological action of these compounds in which the dication first binds in the minor groove of DNA and forms a complex that results in the inhibition of the microbial topoisomerase II enzyme.

Introduction

Dicationic diaryl heterocyclic molecules are effective against a number of microbial infections including *Trypanosoma rhodesience*,[1] *Pneumocystis carinii*,[2] *Giardia lamblia*,[3] and *Cryptosporidium parvum*.[4] The mode of antimicrobial action for these dicationic molecules has been linked to their selective binding to the minor-groove of DNA at AT rich sites and their ability to selectively interfere with the normal functioning of the parasite topoisomerases.[5] Similar studies with both pentamidine analogs and bis-benzimidazole derivatives have demonstrated a strong correlation between DNA minor-groove affinity and antigiardial activity.[3,6] The mechanism of action of these compounds has been postulated to require binding of the componds in the DNA minor-groove, and the resulting complex is thought to be responsible for inhibition of an ATP-dependent giardial topoisomerase.[3]

We reported sometime ago that dicationic 2,5-diarylfurans were quite active against *T. rhodesience* in mice[1] and they were later shown to be effective in a simian model.[7] More recently, it has been shown that certain furan dications interact with DNA by two different and competing binding modes which involve minor-groove interactions at AT sites and intercalation at GC sequences.[8–10] Further, it has been suggested that 2,5-bis(4-imidazolin-2-ylphenyl)furan intercalates effectively into duplex regions of RNA.[10] In view of the strong binding of diarylfuran molecules to the minor-groove of DNA, the wide spectrum of antiparasitic activity of dicationic diaryl heterocycles and the proposed involvement of a type II topoisomerase in the antiparasitic action of dicationic pentamidine analogs and bis-benzimidazole derivatives, we have prepared a series of furans with modifications of the ring size of the 2,5-diarylfurans cationic centers. The influence of structural modifications on the ring system of the cationic center on nucleic acid binding, on topoisomerase II inhibition, and on *in vivo* activity against *P. carinii* has been evaluated. Molecular modeling suggests that the minor-groove binding site can accommodate increases in length of potential groove binders; however, the ability to increase the effective thickness of the small molecules are expected to be limited by the width of the groove at particular sequences. These points have been tested by the synthesis and analysis of the dicationic furans **1**–**7**; the structures of the furans are given Chart **1**.

Chemistry

The synthesis employed for all the dicatioic furans **1**–**7** uses 2,5-bis(4-cyanophenyl)furan[1] as the key intermediate. The transformation of the bis-nitrile into the desired dicationic compounds has been achieved by two approaches. One method converts the bis-nitrile into a bis-imidate ester using classical Pinner methodology followed by reaction with the appropriate diamine.[1] The second approach employs fusion of the bis-nitrile directly with the hydrochloride salt of the appropriate diamine.[11,12] Both manipulations are represented in the generalized Scheme **1**. The furans **1** and **3** were reported earlier and will not be described herein.[1] The

† Georgia State University.
‡ The University of North Carolina at Chapel Hill.
§ The Institute of Cancer Research.
® Abstract published in *Advance ACS Abstracts,* February 15, 1995.

0022-2623/95/1838-0912$09.00/0

Scheme 1[a]

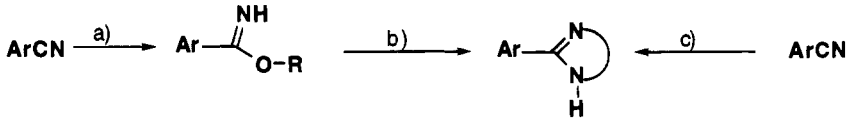

[a] (a) HCl, ROH; (b) $H_2N(CH_2)_nNH_2$; (c) $H_2N(CH_2)_nNH_2$·HCl, heat. Ar = 2,5-bis(4-substituted-phenyl)furan; n = 2, 3, etc.

Chart 1

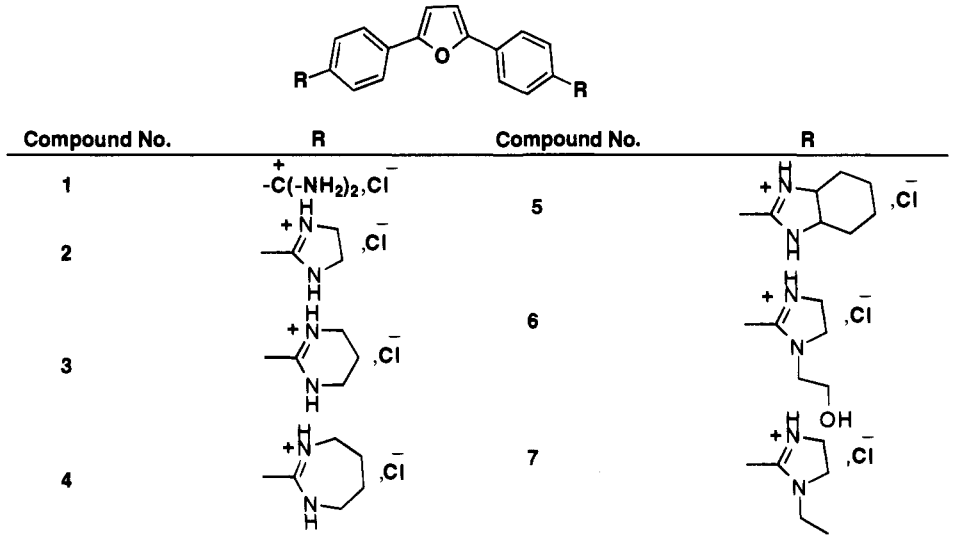

Table 1. Nucleic Acid Binding, Topoisomerase II Inhibition, and Antigiardial Results for Dicationic Diarylfurans

compd	ΔT_m[a] (DNA)	ΔT_m[b] (oligomer)	IC_{50} (μM)[c] *G. l.* Topo II	IC_{50} (μM)[d] *G. l.*
1	25	11.7	0.5–1.0	0.44
2	24	11.4	3–5	1.95
3	>28	13.5	0.5–1.0	0.085
4	>28	10.7	1.5	0.93
5	24.5	5.6	3–6	4.0
6	12.2	1.0	20.0	4.6
7	11.8	1.9	25.0	3.3

[a] Increase in thermal melting of poly(dA·dT), see ref 9. [b] Increase in thermal melting of the oligomer d(GCGCAATTCGCG)$_2$, see ref 12. [c] 50% inhibition of topoisomerase II isolated from *G. lamblia*, see ref 3. [d] 50% inhibition of growth of *G. lamblia* in cell culture, see ref 3.

furan **2** was also previously reported;[1] however, its synthesis by the salt-fusion approach is included in this report.

Biological Results

Table 1 contains thermal melting results from evaluation of the interactions of compounds **1**–**7** with the DNA duplex polymer poly(dA-dT) and with the self-complementary duplex oligomer d(CGCGAATTCGCG)$_2$. The increases in melting temperature on complex formation with the furan dications are related to the binding affinities of these molecules with nucleic acids.[13] The binding to poly(dA-dT) is quite strong for compounds **1**–**4**, and their DNA complexes melt at >90 °C. In order to rank the relative binding affinities for all of the dication interactions with DNA, the duplex oligomer d(GCGCAATTGCGC)$_2$ was employed. The useful temperature range for the oligomer is much wider, allowing measurement of ΔT_m values for the compounds with strong binding affinities. The data from binding studies with the oligomer and **1**–**4** show that these compounds exhibit comparable strong binding affinities: **5** binds with an intermediate affinity and **6** and **7** with relatively low affinity. The extended molecule **5** binds strongly to poly(dA-dT) but with only moderate affinity to the oligomer.

Table 1 also contains results for inhibition of topoisomerase II isolated from *G. lamblia* by **1**–**7**, as well as studies of the inhibition of growth of *G. lamblia* in cell culture. All of the compounds inhibit topoisomerase II isolated from *G. lamblia* at micromolar concentrations and are effective against *G. lamblia* in cell culture. There is a strong correlation between the biological activity of **1**–**7** and their affinity for the AT site in the DNA oligomer as represented by ΔT_m values as well as with their ability to inhibit topoisomerase II (Table 1). Generally, note that compounds which exhibit large ΔT_m values for complex formation with the oligomer also are the most effective against *G. lamblia* in cell culture and are the most potent inhibitors of topoisomerase II. These results support the concept that minor-groove binding to DNA and associated inhibition of topoisomerase are essential components of the biological activity of these dications. Bell et al. have noted similar correlations for the DNA binding of organic dications, topoisomerase II inhibition, and activity against *G. lamblia*.[3,6]

Results from the *in vivo* evaluation of the furan dications on intravenous administration against *P. carinii* in the immunosupressed rat model are presented in Table 2. Data obtained with pentamidine, a compound currently used clinically for treatment of *P. carinii* pneumonia, are included for comparison. Generally, the cyclic amidines **2**–**6** exhibited toxic effects and, with the exception of **3** and **4**, were not effective against *P. carinii*. In contrast, the parent furan **1** clears the infection at quite low dosages and shows significant activity at the 27 nanomolar concentration. The *in vitro* results show that **1**–**4** exhibit comparable behavior with

Table 2. *In Vivo* Activity of Dicationic Diaryl Furans against *Pneumocystis carinii*

compd	dosage[a] (μM/kg/day)	toxicity[b]	cyst/g of lung[c] (% of control)
saline		0	100.0
pentamidine	22.1	+2	3.66
1	13.3	0	2.1
	2.7	0	8.3
	0.27	0	4.8
	0.027	0	55.9
	66.3[d]	0	28.4
2	23.3	+2	35.4
3	10.9	+2	0.4
4	2.3	+3	2.9
	0.18	0	115.4
5	9.2	+1	80.5
6[e]	4.8	+3	107.3

[a] Dosage intravenous except as noted. [b] See ref 2 for detailed explanation of toxicity scale, generally the larger the value the more severe the toxicity, values greater than 2 indicates death of some animals. [c] Counted cysts in a blinding protocol in lung tissue reported as percentage of saline-treated controls, for detailed explanation of experimental error in the method see ref 2. [d] Oral dosage by gavage. [e] Compound **7** was not evaluated against *Pneumocystis carinii*.

the presumed marcomolecular targets; however, from the results with the rat model, it is clear that only the free amidino cationic center, in this series, leads to effective *in vivo* activity. The origin of the toxicity of the "cyclic" amidines is unknown.

The furan **1** is significantly more active and less toxic than pentamidine in the rat model. In view of the effectiveness of **1** by the intravenous route, it seemed prudent to test **1** by using oral dosage. Significant activity and no evidence of toxicity for **1** at the relatively high dosage of 66 μM/kg was observed when it was given orally. Clearly compound **1** is a compound which merits further investigation, and we are developing a wide variety of additional compounds in the furan series.

Structural Analysis

To determine the DNA binding mode for the furans and to probe the molecular basis for the differences in their binding affinities, a crystal structure was obtained for the complex of the amidine **1** with the d(CGCGAATTCGCG)$_2$ duplex (Figure **1**). As can be seen, the compound fits well into the DNA minor-groove and covers the four base pairs of the central AATT binding site of the oligomer duplex. The compound is able to slide deeply into the groove, and close contacts (1.9–2.0 Å) are formed between phenyl protons on the compound and the AC2H protons of A_6 in both strands of the sequence d($C_1G_2C_3G_4A_5A_6T_7T_8C_9G_{10}C_{11}G_{12}$)$_2$. With a GC base pair at the 6 position, the amino group of G would prevent a similar penetration of the compound into the groove. With the compound in this binding site in the groove, one NH_2 group of each amidine points to the floor of the groove and forms a hydrogen bond with the 2-carbonyl group of T_8 on each strand of the duplex. The second NH_2 group of each amidine points away from the floor of the minor-groove, but they both lie between phosphate groups on each strand of the duplex at the outer edge of the minor-groove to provide favorable electrostatic interactions in the complex (Figure **1**).

As observed with the similar minor-groove binding diamidines berenil,[14] pentamidine,[15] and propamidine,[16] the minor-groove in the central AATT sequence is narrow and forms a better binding pocket for the unfused aromatic dications than GC sites would do. The AT specificity, as with the other diamidines,[14–16] arises primarily from three factors: close fit of the compounds into the narrow minor groove in AT sequence regions, close contact between the compound and the C2H proton on A bases, and hydrogen bonds from the amidine groups to the AT base pairs.

As can be seen in Figure **1**, the amidine **1** extends across the four base pairs of the oligomer AATT sequence, and the lower affinity of the extended compound **5** for the oligomer may be a consequence of its extension

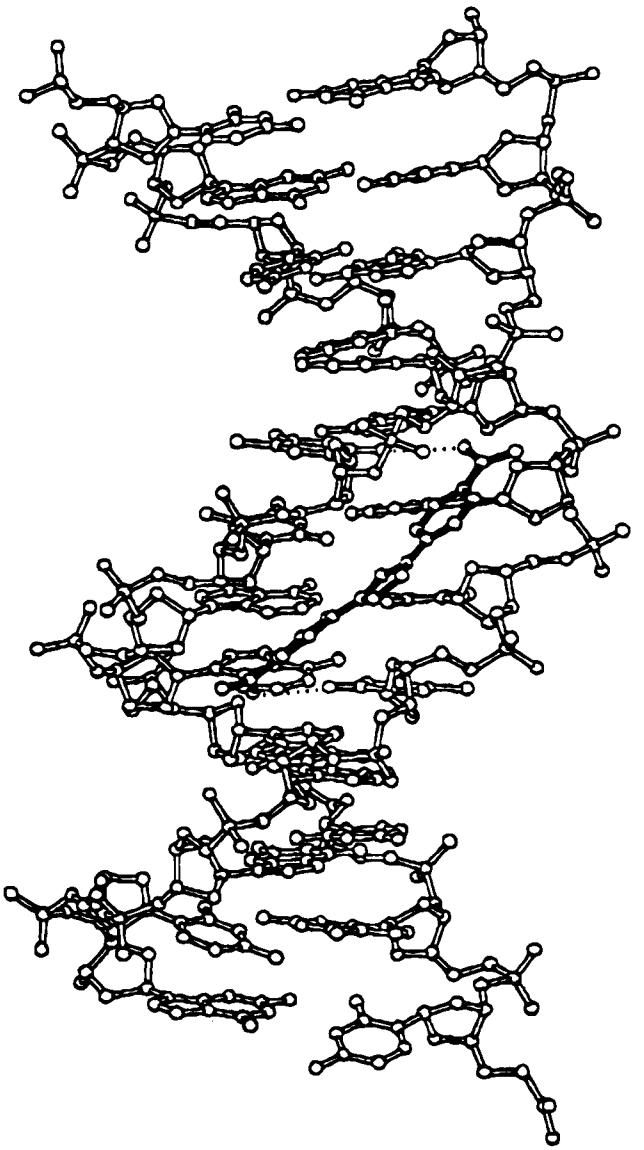

Figure 1. A molecular model of the complex between 1 and d(CGCGAATTCGCG)$_2$ from the crystal structure. The bonds in compound **1** are black while those in the DNA duplex are white. The view is into the minor-groove with **1** located at the AATT site. The 5′ C of one strand (strand A) is at the lower right while the 5′ C of the other strand (strand B) in the figure is at the upper left. A nitrogen of the lower amidine group in the figure is in hydrogen bonding distance to O2 of T_8 on strand B (lower dashed line) while a nitrogen on the upper amidine in the Figure is within hydrogen bonding distance to O2 of T_8 in strand A; with these two H-bonds the DNA strands are reversibly cross-linked. The twist of the diphenylfuran system is easily seen in the view shown and it is complementary to the twist of the minor-groove. In a space-filling view **1** fits quite well into the cavity of the minor groove at the AATT sequence and forms extensive van der Waals contacts with the walls of the groove.

into the GC sequence regions of the duplex. Steric clash with the minor-groove hydrogen bond of GC base pairs could push the compound off the floor of the minor groove and result in the observed weakened binding. Such a clash could not occur in the AT polymer, confirming data that shows that the compound binds relatively more strongly to the polymer. The relatively weaker interactions of the N-substituted imidazolines **6** and **7** are not as easily understood. Compounds **6** and **7** have only a single possible orientation of the substituted imidazoline groups in the DNA complex while the unsubstituted imidazoline has four equivalent configurations. However, this does not appear to be sufficient to account entirely for the dramatic drop in T_m for **6** and **7**. Molecular mechanics calculations predict a torsion angle of approximately 42° between the phenyl groups and the imidazoline rings of **6** and **7**, whereas the similar torsion angle for **2** is near zero. The twist angle between the cationic centers and the phenyl rings may also be a contributor to the reduced T_m values for **6** and **7**. Although, it appears that the added substituents can fit reasonbly well along the outer edge of the minor-groove in a complex such as that shown in Figure **1**. The ethyl or hydroxyethyl substituent of **6** and **7** are close to DNA phosphate groups and may reduce electrostatic interactions between the compound and phosphate or may interfere with phosphate hydration. More detailed modeling and experimental studies are underway to test these ideas.

Experimental Section

Melting points were recorded using a Thomas-Hoover (Uni-Melt) capillary melting point apparatus and are uncorrected. ^{1}H NMR and ^{13}C NMR spectra were recorded employing a Varian GX400 spectrometer, and chemical shifts (δ) are in ppm relative to TMS unless otherwise noted. Mass spectra were recorded on a VG Instruments 70-SE spectrometer (Georgia Institute of Technology, Atlanta, GA). IR spectra were recorded using a Michelson 100 (Bomem, Inc.) instrument. Elemental analysis were obtained from Atlantic Microlab Inc. (Norcross, GA) and are within ±0.4 of the theoretical values. All chemicals and solvents were purchased from Aldrich Chemical Co. or Fisher Scientific.

2,5-Bis[4-(4,5-dihydro-1*H*-imidazol-2-yl)phenyl]furan Dihydrochloride (2). This compound was reported earlier,[1] obtained by the imidate ester; the procedure here illustrates the fusion approach. 2,5-Bis(4-cyanophenyl)furan (0.5 g, 1.9 mmol), ethylenediamine dihydrochloride (4.9 g, 37 mmol), and ethylenediamine (2.5 mL, 37 mmol) were mixed. The mixture was heated at 300–310 °C for 10 min in a sand bath. After cooling, the mixture was dissolved in hot water. Yellow crystals separated on cooling. The compound was recrystallized from boiling water to yield 208 mg (24%) and dried under vacuum at 80 °C for 12 h: TLC ($CHCl_3$:CH_3OH:25% NH_4OH = 11:4:1, one spot); mp >360 °C; ^{1}H-NMR (DMSO-d_6, TMS) δ 4.01 (s, 8H), 7.45 (s, 2H), 8.08 (d, 4H, J = 8.3 Hz), 8.15 (d, 4H, J = 8.3 Hz), 8.15 (d, 4H, J = 8.3 Hz), 10.50 (br s, 4H); ^{13}C-NMR (DMSO-d_6, TMS) δ 45.5, 113.2, 121.6, 125.3, 130.1, 135.8, 153.4, 165.8; IR (KBr) 3412, 3123, 2971, 1608, 1580, 1491, 1367, 1287, 1033, 850, 745, 673 cm^{-1}; MS (M$^+$) 356 (free base). Anal. ($C_{22}H_{20}N_4O$·2HCl·2H_2O) C, H, N.

2,5-Bis[4-(4,5,6,7-tetrahydro-1*H*-1,3-diazepin-2-yl)-phenyl]furan Dihydrochloride (4). The bis-methoxyethanol imidate ester dihydrochloride from 2,5-bis(4-cyanophenyl)-furan (1 g, 0.002 mol) and 1,4-diaminobutane (0.5 g) in 10 mL of 1,2-dimethoxyethane were refluxed for 2 days. The solvent was removed under vacuum, and water was added. The precipitate was filtered, washed with water, and dried in a vacuum oven. The filtrate was neutralized using 2 M sodium hydroxide, and another portion of the free base was obtained. The crude free base was converted into the hydrochloride by hydrogen chloride in methanol. The total yield of free base was 51%: mp >300 °C; ^{1}H-NMR (DMSO-d_6) δ 2.02 (s, 8H), 3.71 (s, 8), 7.38 (s, 2H), 7.86 (d, 4H, J = 8.3 Hz), 8.04 (d, 4H, J = 8.3 Hz), 9.77 (s, 4H); ^{13}C-NMR (D_2O(CH_3)$_3$$SiCH_2CH_2CO_2$-Na) δ 28.0, 47.0, 113.9, 126.5, 129.7, 131.2, 137.0, 154.5, 167.1; IR (KBr) 687, 747, 814, 930, 1331, 1364, 1459, 1597, 3008, 3164 cm^{-1}; MS (EI) (M$^+$) 412 (free base). Anal. ($C_{26}H_{28}N_4O$·2HCl·3.5H_2O) C, H, N.

2,5-Bis[4-(3a,4,5,6,7,7a-hexahydro-1*H*-benzimidazol-2-yl)phenyl]furan Dihydrochloride (5). 1,2-Diaminocyclohexane (9 mL) was treated with ethanolic HCl. The solution was evaporated to dryness, and a another portion of the amine (9 mL) and 2,5-bis(4-cyanophenyl)furan (2 g) were added. The mixture was maintained at 300–310 °C in a sand bath for about 10 min. Progress of the reaction was monitored by TLC ($CHCl_3$:CH_3OH:NH_4OH = 44:8:1, v/v/v). After cooling, the residue was recrystallized from water to afford analytically pure yellow crystals (1.4 g, 36%): mp >300 °C; ^{1}H-NMR (DMSO-d_6, TMS) δ 1.30–2.00 (m, 16H), 4.36 (s, 4H), 7.46 (s, 2H), 8.18 (m, 8H), 10.87 (s, 4H); ^{13}C-NMR (DMSO-d_6, D_2O) δ 18.9, 25.8, 57.0, 112.7, 122.3, 125.0, 130.0, 135.5, 153.4, 153.4, 164.9; IR (KBr) 3413, 2991, 1597, 1501, 1354, 1293, 1016, 930, 853, 796, 747, 676 cm^{-1}; MS (M$^+$) 464 (free base). Anal. ($C_{30}H_{32}N_4O$·2HCl·0.25H_2O) C, H, N.

2,5-Bis[4-(4,5-dihydro-1-(hydroxyethyl)-1*H*-imidazol-2-yl]phenyl]furan Dihydrochloride (6). A mixture of *N*-(2-hydroxyethyl)ethylenediamine (0.64 g, 0.006 mol) in 15 mL of absolute ethanol and the bis-ethyl imidate ester dihydrochloride from 2,5-bis(4-cyanophenyl)furan (0.87 g, 0.002 mol) was heated under reflux for 12 h. The solvent was removed by distillation, and the resulting residue was triturated with ice/water, the pH was adjusted to 10 with 2 M NaOH, and the precipitated solid was filtered, washed with water, dried, and recrystallized from ethanol–ether to yield a light yellow crystalline solid: 0.72 (81%); mp 119–120 °C; IR (KBr) 3390, 3290, 3132, 2864, 1615, 1595, 1421, 1276, 1059, 849 cm^{-1}; ^{1}H-NMR (DMSO-d_6) δ 7.87 (d, 4H, J = 8.3 Hz), 7.64 (d, 4H, J = 8.3 Hz), 7.16 (s, 2H), 3.75 (t, 4H, J = 9.8 Hz), 3.53 (t, 4H, J = 5.8 Hz), 3.47(t, 4H, J = 9.8 Hz), 3.1(t, 4H, J = 5.8 Hz); ^{13}C-NMR (DMSO-d_6) δ 165.8, 152.4, 130.8, 128.7, 123.1, 109.2, 59.3, 52.6, 51.4, 51.1; MS *m/e* 444. The free base (0.45 g, 0.001 mol) was suspended into 10 mL of ethanolic HCl and heated under reflux for 30 min, concentrated under vacuum, and triturated with dry ether, a shining yellow crystalline solid was filtered, and the solid was washed with ether and dried in a vacuum to yield 0.45 g (89%): mp 178–179 °C; IR (KBr) 3407, 3089, 2919, 1615, 1569, 1370, 1288, 1067, 853, 669 cm^{-1}; ^{1}H-NMR (DMSO-d_6/50 °C) δ 10.8 (br s, 2H), 8.9 (d, 4H, J = 8.6 Hz), 7.87 (d, 4H, J = 8.6 Hz), 7.4 (s, 2H), 5.45 (vbr, 2H), 4.18–4.10 (m, 4H), 3.99–3.92 (m, 4H), 3.66–3.5 (m, 4H), 3.48–3.42 (m, 4H); ^{13}C-NMR (DMSO-d_6/50 °C) δ 165.9, 152.3, 133.4, 129.8, 123.7, 121.5, 111.2, 56.6, 49.4, 49.2, 42.5; MS (M$^+$) 444 (free base). Anal. ($C_{26}H_{28}N_4O_3$·2HCl·H_2O) C, H, N.

2,5-Bis[4-(4,5-dihydro-1-ethyl-1*H*-imidazol-2-yl)phenyl]-furan Dihydrochloride (7). To a suspension of the bis-ethyl imidate ester dihydrochloride from 2,5-bis[4-cyanophenyl]-furan (0.65 g, 0.0015 mol) in 10 mL of absolute ethanol was added *N*-ethylenediamine (0.4 g, 0.0045 mol), and the mixture was heated at reflux, under nitrogen, for 12–14 h. The solvent was removed by distillation under vacuum, and the remaining oil was diluted with ice/water and basified with 1 M NaOH to pH 10. A gummy solid separated from the aqueous phase. The solid was washed with water, dried in vacuum, and recrystallized from ethanol–$CHCl_3$ to yield a hygroscopic yellow solid, 0.45 g (73%), MS *m/e* 412. The free base (0.41 g, 0.001 mol) was dissolved in 10 mL of ethanolic HCl and stirred at 35–40 °C for 1 h. The excess solvent was distilled under vacuum, and the resulting semisolid was triturated with dry ether. The ether was removed under vacuum, and the resulting solid was dried under vacuum to yield a very hygroscopic yellow crystalline solid: 0.45 g (93%); mp 163–4 °C dec; ^{1}H-NMR (D_2O/DMSO-d_6) δ 8.08 (d, 4H, J = 8.3 Hz), 7.76(d, 4H, J = 8.3 Hz), 7.26 (s, 2H), 4.24–4.06 (m, 8H), 3.6–3.56 (m, 4H), 1.34 (br t, 6H); ^{13}C-NMR (D_2O/DMSO-d_6) δ 165.0, 154.2, 133.5, 129.3, 123.9, 121.3, 111.3, 48.9, 42.5, 41.7, 12.4. Anal. ($C_{26}H_{28}N_4O$·2HCl·H_2O) C, H, N.

Methods: DNA Thermal Melting. Thermal melting curves for DNA and its complexes with **1**–**7** were determined as previously described[17] by following the adsorption change at 260 nm as a function of temperature. T_m values were determined from the first derivative plots. Compounds are compared by the increase in T_m ($\Delta T_m = T_m$ of complex $- T_m$ of the free nucleic acid) they produce in MES buffer (0.01 M 2-(*N*-morpholino)ethanesulfonic acid, 0.001 M EDTA, 0.1 M NaCl adjusted to pH 6.0) at saturating amounts of compound (a ratio of 0.3 mol of compound to nucleic acid bases) unless otherwise indicated. DNA and complex solutions were as previously described.[17]

Crystallography. The structure of **1**–DNA oligomer complex was determined as previously described,[14-16] and the complete details of the structure determination and the coordinates will be published elsewhere. Crystals of the complex between **1** and d(CGCGAATTCGCG)$_2$ were grown from sitting drops at 286 K. The crystal used for data collection was obtained from a drop containing 4 μL of 40% 2-methylpentane-2,4-diol (MPD), 2.5 μL of 5 mM (**1**), 2 μL of 200 mM $MgCl_2$, 1.5 μL of 2.4 mM spermine, and 4 μL of 3 mM dodecamer equlibrated against a reservoir of 4 mL of 40% MPD for 2 weeks. All solutions were prepared using 30 mM sodium cacodylate buffer at pH 7.0.

The crystal (approximate dimensions 0.5 × 0.3 × 0.15 mm) was mounted in a 0.5 mm Lindemann glass capillary with a small amount of the mother liquor. Intensity data were collected at 287 K using a Siemens-Xentronics multiwire area detector equipped with a rotating anode X-ray generator (40 mA, 70 kV) and graphite monochromator. No crystal decay was apparent.

Merging of the data yielded 3472 unique reflections out of a possible 3895 (89%) with a merging R value of 8.81%. The unit cells dimensions were $a = 25.28$, $b = 40.69$, $c = 66.73$ Å, and the space group $P2_12_12_1$, suggesting a structure isomorphous with the native dodecamer sequence and many related drug complexes. Therefore, for a starting model for the refinement (using X-PLOR 3.1)[18] we used the coordinates of the DNA from the γ-oxapentamidine complex solved in this laboratory.[19] Rigid-body refinement using data in the range 8.0–3.5 Å (871 reflections) gave an R factor of 29.2%. Rigid group refinement with the DNA divided into 70 groups (one for each base, sugar and phosphate) and the same resolution range reduced the R factor to 22.9%. After four rounds of positional refinement, extending the resolution range in stages to 2.2 Å (2475 reflections), and a subsequent round of B factor refinement the R factor was 24.6%. At this stage electron density maps, displayed using the graphics package "O"[20] revealed a clear volume of density in the DNA minor groove which, though not completely continuous, provided a good fit to an energy minimized model for the furan (**1**). Partial charges for the furan were calculated using MOPAC/ESP[21] and other missing force-field parameters were obtained by interpolation. Positional and B factor refinement led to an R factor of 22.9%. In the course of a further 10 rounds of map generation, assignment of solvent (water) positions, positional and B factor refinement, 53 waters were added, and the R factor was reduced to 17.9%.

Acknowledgment. This work was supported by NIH Grant NIAID AI-33363 and CRC Grant SP:384 (to S.N.). An award by the Chemical Instrumental Program of NSF (CHE 8409599) provided partial support for acquisition of the Varian VXR400 spectrometer. We appreciate the technical assistance of W. Brake and B. Bender with the animal model for *Pneumocystis carinii*.

References

(1) Das, B. P.; Boykin, D. W. Synthesis and antiprotozoal activity of 2,5-bis(4-guanylphenyl)furans. *J. Med. Chem.* **1977**, *20*, 531–536.

(2) Tidwell, R. R.; Jones, S. K.; Naiman, N. A.; Berger, L. C.; Brake, W. B.; Dykstra, C. C.; Hall, J. E. Activity of cationically substituted bis-benzimidazoles against experimental *Pneumocystis carinii* pneumonia. *Antimicrob. Agents Chemother.* **1993**, *37*, 1713–1716.

(3) Bell, C. A.; Dykstra, C. C.; Naiman, N. N.; Cory, M.; Fairley, T. A.; Tidwell, R. R. Structure-activity studies of dicationic substituted bis-benzimidazoles against *Giardia lamblia*: Correlation of antigiardial activity with DNA binding affinity and giardial topoisomerase II inhibition. *Antimicrob. Agents Chemother.* **1993**, *37*, 2668–2673.

(4) Blagburn, B. L.; Sundermann, C. A.; Lindsay, D. S.; Hall, J. E.; Tidwell, R. R. Inhibition of *Cryptosporidium parvum* in neonatal Hsd:(1CR)BR swiss mice by polyether ionophores and aromatic amidines. *Antimicrob. Agents Chemother.* **1991**, *35*, 1520–1523.

(5) Dykstra, C. C.; McClernon, D. R.; Elwell, L. P.; Tidwell, R. R. Selective inhibition of topoisomerases from *Pneumocystis carinii* versus topoisomerases from mammalian cells. *Antimicrob. Agents Chemother.* **1994**, *38*, 1890–1898.

(6) Bell, C. A.; Cory, M.; Fairley, T. A.; Hall, J. E.; Tidwell, R. R. Structure-activity relationships of pentamidine analogs against *Giardia lamblia* and correlation of anti giardial activity with DNA binding affinity. *Antimicrob. Agents Chemother.* **1991**, *35*, 1099–1107.

(7) Steck, E. A.; Kinnamon, K. K.; Davidson, D. E.; Duxbury, R. E.; Johnson, A. J.; Masters, R. E. *Trypanosoma rhodesience*: Evaluation of the Antitrypanosomal Action of 2,5-bis(4-Guanylphenyl)-furan Dihydrochloride. *Exp. Parasitol.* **1982**, *53*, 133–144.

(8) Wilson, W. D.; Tanious, F. A.; Barton, H.; Jones, R. L.; Strekowski, L.; Boykin, D. W. Binding of 4′,6-diamidino-2 phenylindole (DAPI) to GC sequences in DNA. *J. Am. Chem. Soc.* **1989**, *11*, 5008–5010.

(9) Tanious, F. A.; Spychala, J.; Kumar, A.; Greene, K.; Boykin, D. W.; Wilson, W. D. Different binding mode in AT and GC sequences for unfused-aromatic dications. *J. Biomol. Struct. Dyn.* **1994**, *11*, 1063–1083.

(10) Wilson, W. D.; Ratmeyer, L.; Zhao, M.; Strekowski, L.; Boykin, D. W. The search for structure-specific nucleic acid-interactive drugs: Effects of compound structure on RNA versus DNA interaction strength. *Biochemistry* **1993**, *32*, 4098–4104.

(11) Oxley, P.; Short, W. F. Amidines. Part I. Preparation of amidines from cyanides. *J. Chem. Soc.* **1946**, 147–150.

(12) Spychala, J.; Boykin, D. W.; Wilson, W. D.; Zhao, M.; Tidwell, R. R.; Dykstra, C. C.; Hall, J. E.; Jones, S. K.; Schinazi, R. F. Synthesis of dicationic diaryltriazines nucleic acid binding agents. *Eur. J. Med. Chem.* **1994**, *29*, 363–367.

(13) Crothers, D. M. Statistical thermodynamics of nucleic acid melting transitions with coupled binding equilibria. *Biopolymers* **1971**, *10*, 2147–2160.

(14) Brown, D. G.; Sanderson, M. R.; Garman, E.; Neidle, S. Crystal structure of a berenil-d(CGCAAATTTGCG) complex: An example of drug-DNA recognition based on sequence-dependent structural features. *J. Mol. Biol.* **1992**, *226*, 481–490.

(15) Edwards, K. J.; Jenkins, T. C.; Neidle, S. Crystal structure of a pentamidine-oligonucleotide complex: Implications for DNA-binding properties. *Biochemistry* **1992**, *31*, 7104–7109.

(16) Nunn, C. M.; Jenkins, T. C.; Neidle, S. Crystal structure of d(CGCGAATTCGCG) complexed with propamidine, a short chain homologue of the drug pentamidine. *Biochemistry* **1993**, *32*, 13838–13845.

(17) Kibler-Herzog, L.; Kell, B.; Zon, G.; Shinnozuka, K.; Mizan, S.; Wilson, W. D. Duplex Stabilities of Phosphorothioate, Methylphosphonate and RNA Analogs of two DNA 14-mers. *Nucleic Acids Res.* **1990**, *18*, 3545–3555.

(18) Brunger, A. T.; Kuriyan, J.; Karplus, M. Crystallographic R-factor Refinement by Molecular Dynamics. *Science* **1987**, *235*, 458–460.

(19) Nunn, C. M.; Jenkins, T. C.; Neidle, S. Crystal Structure of γ-Oxapentamidine Complexed with d(CGCGAATTCGCG)$_2$: The Effects of Drug Structural Change on DNA Minor Groove Recognition. *Eur. J. Biochem.* **1994**, in press.

(20) Jones, T. A.; Zhou, J.-Y.; Cowan, S. W.; Kjeldgaard, M. Improved Methods for Building Models in Electron Density Maps and the Location of Errors in these Models. *Acta Crystallogr.* **1991**, *A47*, 110–119.

(21) Stewart, J. P. P. Mopac 6.0 (QCPE), available from the Quantum Chemistry Program Exchange, Indiana University, Bloomington, IN 47405.

JM940698P